

NUCLEAR STRUCTURE -- THEORY

A SIMPLE RELATION FOR ALPHA DECAY HALF LIVES

B. A. Brown

The earliest law for the systematics of α decay lifetimes was formulated by Geiger and Nuttall.¹ This was the observation that $\text{Log}_{10} T_{1/2}(\text{sec})$ plotted vs $1/\sqrt{Q_\alpha}$, where Q_α is the α decay Q value, empirically formed straight lines for a series of nuclei with the same charge number. In Fig. 1a, I show

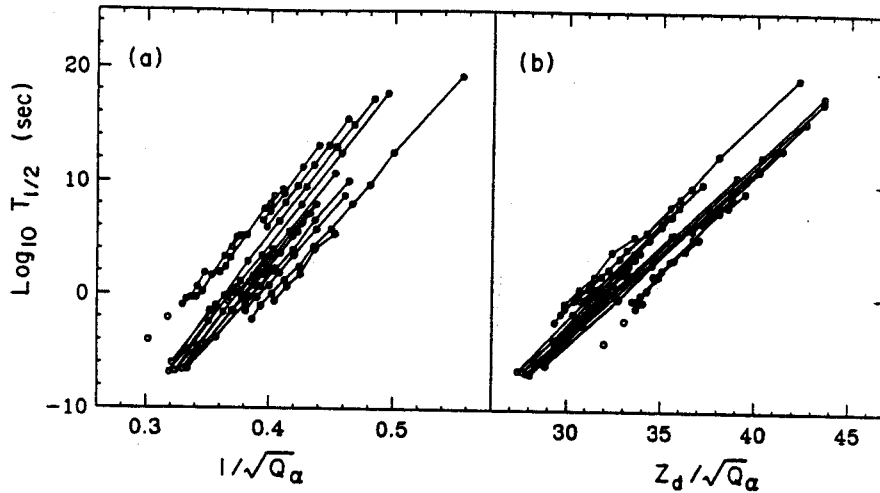


Figure 1: On the left-hand side (a), the experimental values for $\text{Log}_{10} T_{1/2}(\text{sec})$ are plotted vs $1/\sqrt{Q_\alpha}$, where the data for $T_{1/2}$ and Q_α are taken from Ref 2. On the right-hand side (b), the experimental values for $\text{Log}_{10} T_{1/2}(\text{sec})$ are plotted vs $Z_d/\sqrt{Q_\alpha}$. The points for a given value of Z_d are connected by a line.

a modern version of this plot for the $J_i^\pi = J_f^\pi = 0^+$ α decay data tabulated in Ref 2. There are 119 data points for a range of Z_d from 74 to 106, where Z_d is the charge number of the daughter nucleus. Even though the data for a given Z_d value fall on roughly a straight line, there is a large scatter between the lines for different Z_d values.

It is well known that this trend can be understood in terms of the semi-classical approximation for the decay rate $W = PW_c T$, where P is the preformation probability, W_c is the collision rate of the α particle with the nuclear surface, and T is the barrier penetration factor given for $\ell=0$ decays in the WKB approximation by

$$T = \exp\left\{-2 \int_{R_i}^{R_c} \sqrt{2\mu[V(r) - Q_\alpha]}/\hbar^2 \cdot dr\right\}. \quad (1)$$

In this expression R_i is the "touching" radius, $R_i = R_\alpha + R_d$, where R_α and R_d are the hard-sphere radii

for the α and daughter nuclei, respectively. The potential is given by $V(r) = Z_\alpha Z_d e^2 / r$, where $Z_\alpha = 2$, and R_c is the classical turning point, $R_c = Z_\alpha Z_d e^2 / Q_\alpha$. The reduced mass is $\mu = M_\alpha M_d / (M_\alpha + M_d)$. Eq. (1) can be integrated exactly to give

$$T = \exp\{-2Z_\alpha Z_d e^2 \sqrt{2\mu/Q_\alpha \hbar^2} [\cos^{-1}(x) - x\sqrt{1-x^2}]\}, \quad (2)$$

where $x = \sqrt{R_t/R_c}$. The last part of Eq. (2) can be expanded in a power series in x :

$$[\cos^{-1}(x) - x\sqrt{1-x^2}] = (\pi/2) - 2x + x^3/3 \dots \quad (3)$$

The x^3 term is usually dropped in the discussion of this expansion, but it is important at the level of about one order of magnitude in the half-life. The next order term in x^5 is not important at the present level of experimental and theoretical uncertainty. The barrier penetration factor in terms of the power series expansion is

$$T = \exp\{-2\sqrt{2\mu/\hbar^2} \left[\frac{\pi Z_\alpha Z_d e^2}{2\sqrt{Q_\alpha}} - 2\sqrt{Z_\alpha Z_d e^2 R_t} + \frac{Q_\alpha R_t^{3/2}}{3\sqrt{Z_\alpha Z_d e^2}} \right]\}. \quad (4)$$

The original Geiger-Nuttall rule emerges from the first term in this expansion together with the fact that the second term does not depend on Q_α . Further, as previously noted,³ this result suggests that $\text{Log}_{10} T_{1/2}(\text{sec})$ vs $Z_d/\sqrt{Q_\alpha}$ may be a better way to plot the data. The result is shown in Fig. 1b, where the data again form lines for a fixed Z_d value, and where the scatter as a function of Z_d is somewhat less than in Fig. 1a. The scatter in Figs. 1a and 1b is due mainly to the second term on the left-hand side of Eq. (4).

Here I point out that there is an interesting interpolation between Figs. 1a and 1b. Namely, if one plots $\text{Log}_{10} T_{1/2}$ vs $Z_d^{0.6}/\sqrt{Q_\alpha}$ as shown in Fig. 2a, the points fall on a nearly universal straight line. Also shown in this figure is a straight line which represents a best fit to the data. It is given by $\text{Log}_{10} T_{1/2}(\text{sec}) = (9.54 Z_d^{0.6}/\sqrt{Q_\alpha}) - 51.37$, where Q_α is expressed in units of MeV. The rms deviation of the experimental values of $\text{Log}_{10} T_{1/2}(\text{sec})$ from this straight line is 0.33. The rms deviation of the straight-line fit as a function of the power of Z_d has a sharp minimum at a value of about 0.6.

It is not obvious that this should follow from Eqs. (1), however, numerically it does. In Fig. 2b I show $\text{Log}_{10} T_{1/2}(\text{sec}) = \text{Log}_{10}(\ln 2/W)$ vs $Z_d^{0.6}/\sqrt{Q_\alpha}$ where W is calculated from Eq. (999) and the experimental

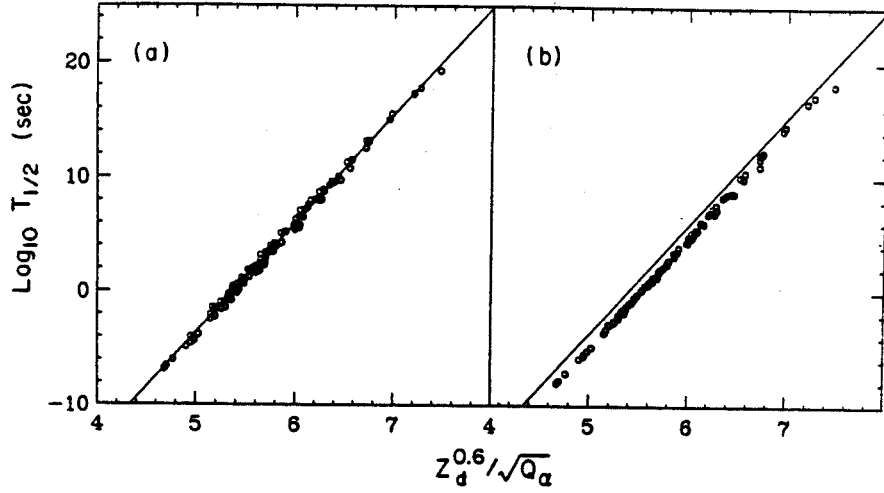


Figure 2: On the left-hand side (a), the experimental value for $\text{Log}_{10} T_{1/2}(\text{sec})$ are plotted vs $Z_d^{0.6}/\sqrt{Q_\alpha}$. The straight line represents a best fit to the data. On the right-hand side (b), the theoretical values for $\text{Log}_{10} T_{1/2}(\text{sec})$ from Eq. (999) are plotted vs $Z_d^{0.6}/\sqrt{Q_\alpha}$ and compared to the best fit line from Fig. 2a.

Q_α are used. The theoretical results are compared to the best fit line from Fig. 2a. I have used $P = 1$, $R_\alpha = 2.15 \text{ fm}$, $R_d = r_o A_d^{1/3}$ with $r_o = 1.2 \text{ fm}$, and the classical value for W_c given by

$$W_c = (1/2R_t)\sqrt{2Q_\alpha/\mu}, \quad (5)$$

which follows from the classical motion of an α particle in the nucleus in a potential $V(r) = 0$ for $r < R_t$. (The results are, however, relatively insensitive to the value assumed for $V(r)$ inside the nucleus.) The radii R_α and R_d used above are the uniform sphere radii which are related to the rms charge radii, r_{ch} by $R = \sqrt{5/3} r_{ch}$ ($r_{ch} = 1.67 \text{ fm}$ for the α particle). The theoretical points from the semi-classical WKB approximation follow the straight line dependence even a little better than the data (rms=0.20). Other simple relations which have been proposed which are similar in spirit to mine but not the same in form. These are summarized in Ref 4. In particular, the form of Waptra et al.⁵ can be fitted to the data set considered here with the result, $\text{Log}_{10} T_{1/2}(\text{sec}) = [(1.001Z_d + 51.89)/\sqrt{Q_\alpha}] - 51.37$, and with an rms deviation of 0.31. The form of Taagepera and Nurmia⁶ and Keller and Munzel⁷ can be fitted to the data set considered here with the result, $\text{Log}_{10} T_{1/2}(\text{sec}) = 1.598[(Z_d/\sqrt{Q_\alpha}) - Z_d^{2/3}] - 19.94$, and with an rms deviation of 0.33. These systematics should be useful for extrapolations to more exotic nuclei and to superheavy nuclei.

References

1. H. Geiger and J. M. Nuttall, *Phil. Mag.* 22, 613 (1911); H. Geiger, *Zeits. Physik* 8, 45 (1921).
2. B. Buck, A. C. Merchant and S. M. Perez, *Phys. Rev. Lett.* 65, 2975 (1990); *J. Phys.* G17, 1223 (1991).
3. For example: S. S. M. Wong, "Introductory Nuclear Physics" (Prentice Hall, 1990).
4. D. N. Pomenaru and M. Ivascu, *J. Physique* 44, 791 (1983).
5. A. H. Wapstra et al. in "Nuclear Spectroscopy Tables", (North-Holland, Amsterdam) 1959.
6. R. Taagepera and M. Nurmi, *Ann. Acad. Sci. Fenn. Ser. A78*, (1961).
7. K. A. Keller and H. Z. Munzel, *Z. Physik* 255, 419 (1972).

β^+ GAMOW-TELLER STRENGTH IN NUCLEI

B. A. Brown and N. Auerbach^a

We have addressed the question of the relatively large quenching observed for the S_+ strength (in nuclei with $N > Z$) relative to the single-particle jj coupled shell-model estimate, in particular for ^{26}Mg , ^{54}Fe and ^{56}Ni . We explore the interrelationships between various approximations for the model spaces beyond the jj coupling limit, some aspects for the first time. The role of $2p - 2h$ ground-state correlations within a major shell (i.e. the sd shell or pf shell) is reexamined. We find that the QRPA and $2p - 2h$ shell-model calculations (carried out with the same residual interaction) give essentially the same result for the total S_+ strength, whereas the splitting and fine-structure of the strength is realistic only in the shell-model calculation. We also consider correlations beyond $2p - 2h$ by calculating the strength for the case of ^{26}Mg in the sd shell where the full major-shell basis can be included. For this sd case we find about a factor of two additional quenching relative to the $2p - 2h$ model space. The implication of this additional quenching is explored with regard to the transition between jj and $SU(3)LS$ coupling and the associated quadrupole collectivity which can be observed in the the low-lying 0^+ to 2^+ B(E2) values. We find that ^{26}Mg is close to the $SU(3)$ limit whereas ^{54}Fe and ^{56}Ni are closer to the jj limit. Our final values for the total S_+ strength (which includes in addition the global quenching factor of 0.6 due in part to the $2p - 2h$ correlations outside of the major shell) are in good agreement with experiment for ^{26}Mg and ^{54}Fe . The very small GT matrix element obtained from the $2p - 2h$ shell-model calculation for the beta decay of ^{56}Ni to the 1.72 MeV state in ^{56}Co is in qualitative agreement with experiment. 1

The computations were done using the shell-model code OXBASH 2. In order to examine the sensitivity of the results to the truncation of the shell-model space we have performed analogous calculations also for the $^{26}\text{Mg} \rightarrow ^{26}\text{Na}$ GT_+ transitions. In this case, however, it was possible to perform a completely unrestricted shell-model calculation within the sd shell. For the pf shell we use the MSOBEP 3 interaction with the single-particle energies adjusted to reproduce the lowest (single-particle) states in ^{55}Ni and ^{57}Ni under the assumption of a closed-shell configuration for these states. For the sd shell we use the Brown-Wildenthal USD 4 interaction. The RPA and QRPA calculations discussed below were carried out with the USD and MSOBEP interactions for both the RPA and BCS components of the calculations. The BCS was carried out exactly with state-dependent pairing gaps. In addition the RPA and QRPA include explicitly the rearrangement terms for the single-particle energies (such rearrangement terms are

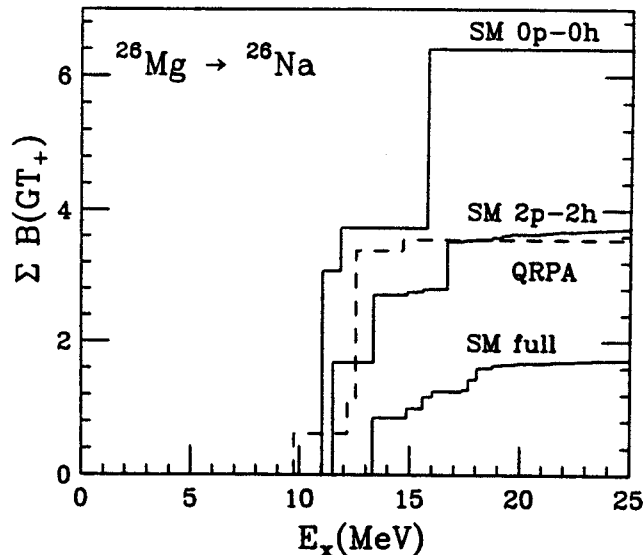


Figure 1: Running sum of the $B(GT_+)$ values for ^{26}Mg vs. excitation energy. S_+ is the total value at $E_x=25$ MeV. The labels correspond to the headings in Table 1.

included implicitly in the shell-model calculations.)

Our extended shell-model calculations for ^{54}Fe and ^{56}Ni are carried out in a space that contains up to $2p - 2h$ configurations, and not the full pf shell space. What would be the effect of an enlarged configuration space beyond $2p - 2h$ states? It is practically impossible, at the present, to provide a direct answer by performing a full calculation in the pf shell. One can however get some guidance from a the full shell-model calculation of the GT transition $^{26}\text{Mg} \rightarrow ^{26}\text{Na}$. In Fig. 1, we show the calculated GT_+ strength for $A = 26$ case for various stages of shell-model approximations and for the pnQRPA. We note that in the full SM model space, an additional (almost a factor of two) quenching of GT_+ strength occurs relative to the $2p - 2h$ calculation.

We use the sd shell results as guidance for the pf shell by considering its relationship to the transition between jj to $SU(3)LS$ coupling and the associated change in quadrupole collectivity. In the $SU(3)LS$ limit the GT_+ strength is zero [since all of the GT strength resides in a single GT_- transition which exhausts the $3(N - Z)$ sum rule] and the quadrupole collectivity [the $B(E2)$ value connecting the ground state and first 2^+ state in ^{26}Mg] is at or near its maximum possible value. This relationship is illustrated in Fig. 2, where the ratio of S_+ to the $0p - 0h$ SM estimate, R_+ , is plotted vs the $B(E2, 2^+ \rightarrow 0^+)$ value. The points (circles) in Fig. 4 correspond to the $0p - 0h$, $2p - 2h$, full and $SU(3)$ -limit values as a function of increasing $B(E2)$ [decreasing R_+]. There is seen to be a simple monotonic relationship between

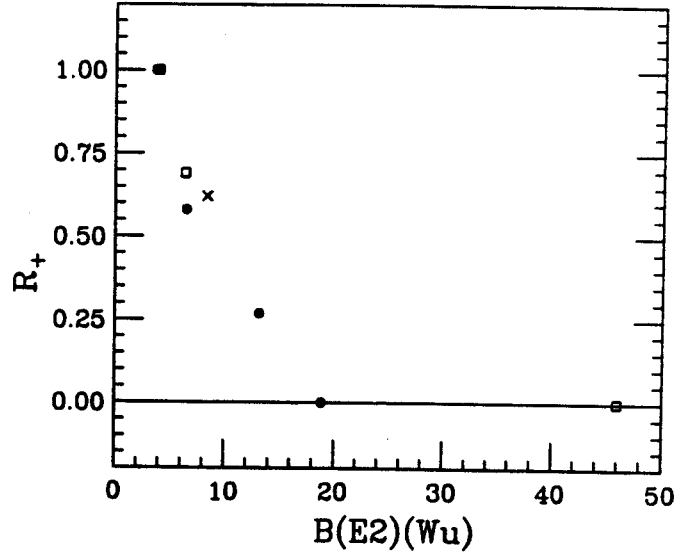


Figure 2: R_+ vs $B(E2)$ for the $0p - 0h$, $2p - 2h$, full and $SU(3)$ -limit calculations for ^{26}Mg (filled circles), and the $0p - 0h$, $2p - 2h$ and $SU(3)$ -limit calculations for ^{54}Fe (squares). The cross corresponds to the experimental $B(E2)$ value for ^{54}Fe . See text for details.

R_+ and $B(E2)$ which is about linear between the $2p - 2h$ and $SU(3)$ -limit values. The $B(E2)$ in the $SU(3)$ limit was obtained by using an $SU(3)$ conserving Hamiltonian 5 for the full-basis SM calculations and is in agreement with the value obtained from the analytical formulae. 6 The experimental $B(E2)$ value for ^{26}Mg 7 is in good agreement with the full sd SM (USD-interaction) value. We can now add to Fig. 4 the $2p - 2h$ and $SU(3)$ -limit values for ^{54}Fe (squares). The experimental $B(E2)$ for ^{54}Fe 7 falls at the point indicated by the cross in Fig. 4, where we have arbitrarily chosen a reasonable interpolated value value of $R_+ = 0.62$ for this point. The S_+ values resulting from this interpolation are given in the column headed "SM full" in Table 1 [we assume the same R_+ value for ^{56}Ni].

The type of quenching discussed up to this point is only due to correlations with the valence major-oscillator shell (sd or pf) and has little affect the $3(N - Z)$ sum rule for the low-lying states. In order to be able to compare to experiment one must take into account the more universal quenching that affects the $3(N - Z)$ sum rule for low-lying states. This can be done by introducing an effective GT transition operator $g_A(\text{eff}) = \sqrt{0.6} g_A$. These numbers for the full shell-model case are shown under the column labeled "full SM(eff)" of Table 1. For the $^{54}\text{Fe} \rightarrow ^{54}\text{Mn}$ and $^{26}\text{Mg} \rightarrow ^{26}\text{Na}$ transitions, the S_+ strengths obtained in the extended shell model are in the range of experimental values given in the last column of Table 1.

Table 1: Calculated S_+ values

AZ	SM $0p-0h$	SM $2p-2h(r)$ (a)	SM $2p-2h$ (b)	RPA or QRPA	SM full	SM full(eff) (c)	Exp
^{26}Mg	6.4	3.38	3.72	2.84	1.72	1.03	1.3 ± 0.6 (e), 0.84 (f)
^{54}Fe	10.29	6.68	7.05	6.70	6.4(d)	3.8(d)	3.1 ± 0.6 (g)
^{56}Ni	13.71	9.81	10.38	10.27	8.5(d)	5.1(d)	

a) $(d_{5/2}, d_{3/2})$ model space for ^{26}Mg and $(f_{7/2}, f_{5/2})$ model space for ^{54}Fe and ^{56}Ni .

b) $(d_{5/2}, d_{3/2}, s_{1/2})$ model space for ^{26}Mg and $(f_{7/2}, f_{5/2}, p_{3/2}, p_{1/2})$ model space for ^{54}Fe and ^{56}Ni .

c) Estimates based on the ^{26}Mg calculation (see text).

d) $g_A(\text{eff}) = \sqrt{0.6} g_A$.

e) From the (p, ι) data of Ref. 8.

f) From the (n, p) data of Ref. 9.

g) From the (p, n) and (n, p) data of Ref. 10.

a. Permanent address: Tel-Aviv University, Tel-Aviv, Israel

References

1. B. Sur et al., Phys. Rev. C42 (1990), 573.
2. A. Etchegoyen, W.D.M. Rae, N.S. Godwin, W.A. Richter, C.H. Zimmerman, B.A. Brown, W.E. Ormand and J.S. Winfield, MSU-NSCL report #524 (1985).
3. W.A. Richter, M.G. Van der Merwe, R.E. Julies and B.A. Brown, Nucl. Phys. A523 (1991), 325.
4. B. A. Brown and B. H. Wildenthal, Ann. Rev. Nucl. Part. Phys. 38 (1988), 29.
5. M. Harvey, Adv. Nucl. Phys. 1 (1968) 67.
6. J. P. Elliott, Proc. Roy. Soc. (London), A245 (1958), 128 and 562.
7. P. M. Endt, At. Data and Nucl. Data Tables 23 (1979), 3 adn 547.
8. R. Madey et al., Phys. Rev. C35 (1987), 2011; C36 (1987), 1647.
9. S. Yen, Can. Jour. Phys. 65 (1987), 595.
10. M.C. Vetterli, et.al, Phys. Rev. Lett. 59 (1987), 439; M.C. Vetterli, et.al, Phys. Rev. C40 (1989), 559.

EFFECTIVE INTERACTIONS FOR THE $0p1s0d$ SHELL-MODEL SPACE

B.A. Brown and E. K. Warburton^a

New shell-model interactions have been constructed in the cross-shell model space connecting the $0p$ and $1s0d$ shells with due regard for the perturbative effects of the neighboring $0s$ and $0f1p$ shells. The interactions have three distinctive $0p$ -shell, cross-shell and $1s0d$ -shell parts. The latter was taken to be the previously determined W interaction. The $0p$ -shell interaction was represented by two-body matrix elements and the cross-shell by either a potential or by two-body matrix elements. The interactions are determined by least-squares fits to 51 $0p$ -shell and 165 cross-shell binding energies. It was found that the addition of monopole terms to a potential which was otherwise similar to that of the Millener-Kurath interaction, results in a great improvement in the fit. In the fit to two-body matrix elements, 45 of 97 possible linear combinations of parameters were varied and the root-mean-square deviation for the 165 cross-shell energies was 330 keV. The methods, background and assumptions related to this new interaction are discussed in the following.

Much progress has been made in recent years on our understanding of nuclear states which, to a good approximation, have all active nucleons in a single one of the first four major shells, i.e., $0s$, $0p$, $1s0d$, and $0f1p$. Most notable has been the great success of effective interactions obtained by least-squares fitting experimental binding energies to single-particle energies (SPE) and either two-body matrix elements (TBME) or the parameters of a potential. The classic fit to the $0p$ shell which illustrated the power of this method was made by Cohen and Kurath¹ in 1965. Results for the $1s0d$ shell were obtained by Wildenthal and colleagues^{2,3,4,5,6}. In the earlier of these studies, the interaction was mass independent and separate fits were made to the lower and upper half of the $1s0d$ shell. An important advance made by Wildenthal⁴ in building the W interaction⁶ was to scale the TBME as $(A/18)^{-p_A}$ with $p_A = 0.3$. With this assumption it was finally possible to obtain a good fit to the entire $1s0d$ shell. Subsequently it has been found that the $0p$ shell fit — originally made¹ with mass independent SPE — is better if the interaction is assumed to scale as $(A/16)^{-0.17}$ ⁷. The number of TBME for the $0p$ shell and $1s0d$ interactions are 15 and 63. These numbers are small enough compared to the body of experimental data so that a least-squares fit can be made with the TBME as variables. However the TBME are not all well determined since some do not have a strong dependence on the low-lying level energies. Thus, an important advance in the $1s0d$ study of Chung and Wildenthal³ was the utilization of the linear combination method (LC) — also

termed the direct combination method (DCM)⁸ — in which the error matrix representing the relationship of the TBME to the level energies is diagonalized thus giving linear combinations which are independent of each other^{3,5,8}. Then only those linear combinations of parameters which are well determined (by some external criterion) are varied, the remaining being frozen at some “background” value. The method of least-squares fitting with TBME and SPE as parameters was termed the model-independent (MI) method by Brown, Richter, Julies, and Wildenthal⁵, hereafter referred to as BRJW. Here we have described the MI-LC method.

There are two criteria which can be used to judge these empirical $0p$ and $1s0d$ interactions. First, are the resulting wave functions realistic so that other observables can be predicted reliably? Second, are the empirical interactions in satisfactory agreement with our fundamental understanding of nuclei and the nucleon-nucleon interaction? These empirical interactions meet both criteria with astonishing success. An example of the predictive power for other observables is the study of $M1$ and Gamow-Teller observables in the $1s0d$ shell by Brown and Wildenthal^{6,9}. As for the second criteria, the TBME of the Cohen-Kurath and W interactions are in remarkably good agreement⁵ with the “bare G -matrix plus core-polarization” TBME obtained by the Kuo-Brown method^{10,11}. It is these Kuo-Brown TBME that Wildenthal used for “background” in his application of the MI-LC method in obtaining the W interaction.

For the major shells above mass 40 it is more difficult to make a least-squares fit with the TBME and SPE as parameters because of the larger number of TBME (195 for the $0f1p$ shell) and a lack of sufficient data. A practical alternative is to represent the interaction by a potential and vary its parameters. This will result in a more and more constrained fit as the dimensions of the model space increase. In the $0p$ shell the 15 TBME can be formally replaced by a 15-parameter two-body LS potential so that fitting to the TBME or to this potential gives identical results¹. But in higher shells the use of a potential with a limited number of parameters offers an attractive alternative to the MI-LC method of constraint. We refer to the use of a potential as the model-dependent (MD) method. The use of a one-boson-exchange potential (OBEP) plus core-polarization correction terms of the multipole-multipole type to describe $1s0d$ nuclei was exhaustively studied by BRJW. The method has been applied to the $0f1p$ ¹² and $0p$ ⁷ shells. These results illustrate the power of the method.

There has been less progress in our understanding of cross-shell states in these nuclei; i.e., states which have active nucleons in more than one major shell. Important steps in our understanding of these

states are the classic particle-hole calculations of Elliot and Flowers ¹³ for ¹⁶O and of Halbert and French ¹⁴ for ¹⁵N. These calculations used a schematic central particle-hole interaction. They demonstrated that the low-lying non-normal parity states of these nuclei were well described by a $1\hbar\omega$ excitation of the $(0s_{1/2})^4(0p)^{4-4}$ configuration. Calculations of this type culminated in the successful and oft-used Millener-Kurath (MK) interaction connecting the 0p and 1s0d shells ¹⁵. The 80 $1\hbar\omega$ “cross-shell” TBME of this interaction were generated from a potential (OBEP) containing central, tensor and spin-orbit terms with a single Yukawa radial form for each. The form of the potential and the strengths of the various terms were carefully chosen from consideration of previous studies — such as those of Refs. ^{13,14} — and of excitation energies of non-normal parity states in $A = 15$ and 16 nuclei, and from a desire to stay close to the form and strength of Kuo’s bare G-matrix potential ¹⁰. When used in conjunction with the Cohen-Kurath 0p-shell interaction ¹ and the W interaction ⁴ — or one of its precursors ^{2,3} — the MK interaction has given us a quite successful description of $2\hbar\omega$ and $3\hbar\omega$ states in $A = 10-22$ nuclei as well as the $1\hbar\omega$ states for which it was originally designed. This success implies the weak-coupling of the 0p and 1s0d shells which, in fact, was anticipated by the very simple calculations of Talmi and Unna ¹⁶. Indeed shell-model calculations explicitly formulated as weak-coupling of these major shells have given very successful descriptions of nuclei near ¹⁶O. In particular we note the elegant formulation of Ellis and Engeland ¹⁷ and the many successful calculations made with it ¹⁸. The weak-coupling approach of Ellis and Engeland has attractive features, the most notable being the sizable reduction in the dimensions of the diagonalizations. The weak-coupling approach is probably the most practical for cross-shell calculations above the 0f1p shell, but with present-day computer resources this reduction is not an important consideration for the lighter nuclei.

The original motivation for the present study was the desire for an effective cross-shell interaction for the 0p1s0d shells of the MK type but with a more complex cross-shell potential with more quantitatively determined parameters and therefore, hopefully, more accurate wave functions. As this study progressed it became clear that an equally accurate and physically meaningful interaction could be obtained by the MI-LC method. Construction of both types of interactions will be described. The bulk of the computations described herein were carried out with the shell-model code OXBASH ¹⁹. With Oxbash, spurious center-of-mass motion is removed by the usual method ²⁰ of adding a center-of-mass Hamiltonian H_{cm} to the interaction. Anticipated uses of the interactions include, e.g., binding energies and Gamow-Teller β decay

rates for neutron-rich nuclei, first-forbidden β decay observables ²¹, and parity non-conservation ^{22,23}.

a. Brookhaven National Laboratory, Upton, New York, 11973.

References

1. S. Cohen and D. Kurath, Nucl. Phys. 73, 1 (1965).
2. B. M. Preedom and B. H. Wildenthal, Phys. Rev. C 6, 1633 (1972).
3. W. Chung, PhD thesis, Michigan State University, 1976.
4. B. H. Wildenthal, Prog. Part. Nucl. Phys. 11, 5 (1984).
5. B. A. Brown, W. A. Richter, R. E. Julies, and B. H. Wildenthal, Anns. Phys. (NY) 182, 191 (1988).
6. B. A. Brown and B. H. Wildenthal, Ann. Rev. Nucl. Par. Sci. 38, 29 (1988).
7. R. E. Julies, W. A. Richter, and B. A. Brown *to be published*.
8. P. J. Brussard and P. W. M. Glaudemans, "Shell-model applications in nuclear spectroscopy", North-Holland, Amsterdam (1977).
9. B. A. Brown and B. H. Wildenthal, Atomic Data Nucl Data Tables 33, 347 (1985).
10. T. T. S. Kuo, and G. E. Brown, Nucl. Phys. 85, 40 (1966).
11. T. T. S. Kuo, Nucl. Phys. A103, 71 (1967); J. Shurpin, T. T. S. Kuo, and D. Strottman, Nucl. Phys. A408, 310 (1983).
12. W. A. Richter, M. G. Van der Merwe, R. E. Julies, and B. A. Brown, Nucl. Phys. A523, 325 (1991).
13. J. P. Elliott and B. H. Flowers, Proc. Royal Soc A 242, 57 (1957).
14. E. C. Halbert and J. B. French, Phys Rev. 105, 1563 (1957).
15. D. J. Millener and D. Kurath, Nucl. Phys. A255, 315 (1975).
16. I. Talmi and I. Unna, Ann. Rev. Nucl. Sci. 10, 353 (1960).
17. P. J. Ellis and T. Engeland, Nucl. Phys. A144, 161 (1970).
18. T. Engeland and P. J. Ellis, Nucl. Phys. A181, 368 (1972). ;S. Lie, T. Engeland, and G. Dahll, Nucl. Phys. A156, 449 (1970). ;S. Lie and T. Engeland, Nucl. Phys. A169, 617 (1971). ;S. Lie, Nucl. Phys. A181, 517 (1972).
19. B. A. Brown, A. Etchegoyen, W.D.M. Rae, and N. S. Godwin, OXBASH, 1984 (unpublished).
20. D. H. Glockner and R. D. Lawson, Phys. Lett. 53B,313 (1974).
21. E. K. Warburton, J. A. Becker, B. A. Brown, and D. J. Millener, Anns. Phys. (N.Y.) 187, 471 (1988).
22. E. G. Adelberger, and W. C. Haxton, Ann. Rev. Nucl. Sci. 35,501 (1985).
23. B. A. Brown, W. A. Richter, and N. S. Godwin, Phys. Rev. Lett. 45, 1681 (1980).

LARGE BASIS SHELL-MODEL TREATMENT OF $A = 16$

B. A. Brown, E. K. Warburton^a and D. J. Millener^a

The light nuclei have always been and will continue to be the premier testing ground for our views on the structure of nuclei. Here we are concerned with $A = 16$ nuclei. ^{16}O has a fascinating and complex structure since $0\hbar\omega$, $2\hbar\omega$, and $4\hbar\omega$ excitations are manifestly apparent amongst the low-lying levels. The $(0+2+4)\hbar\omega$ model of Brown and Green¹ was an early, successful, and important description of these states. From a present-day point of view the Brown-Green model can be described as schematic. Nevertheless, the essential truth remains as was emphasized in a recent study² similar to this one and as will also be reaffirmed here.

We are interested in a microscopic shell-model description of $(0+2+4)\hbar\omega$ excitations in ^{16}O . There are two severe problems encountered in mixed $(0+2+\dots)\hbar\omega$ calculations which we illustrate by a discussion of mixing between $0\hbar\omega$ and $2\hbar\omega$ alone. These are (a) the difficulty of obtaining the mixing between the different $n\hbar\omega$ configurations correctly, and (b) the difficulty of respecting the Hartree-Fock condition *viz-a-viz* one-particle–one-hole (1p-1h) excitations through two oscillator shells. The first of these problems is the most difficult. As has been commented on at length^{3,4,5,6} it has its basic cause in the fact that the low-lying $n\hbar\omega$ states interact most strongly with those higher-lying $(n+2)\hbar\omega$ states which mix via the (20) SU3 tensor part of the $2\hbar\omega$ interaction $V^{2\hbar\omega}$ and are thereby depressed by a considerable amount; ~ 10 MeV in ^{16}O . For example, the $2\hbar\omega$ (20) states commence ~ 20 MeV above the $0\hbar\omega$ ground state so that after the mixing they commence at ~ 30 MeV. Mixing of $(n+4)\hbar\omega$ is needed to restore the proper energy relationship between the $n\hbar\omega$ and $(n+2)\hbar\omega$ states. Hence truncation of the slowly-varying series $n\hbar\omega$, $(n+2)\hbar\omega$, ... will badly distort the relative energies of the different $n\hbar\omega$ configurations and thereby give incorrect mixing between them. Here we explore three approximations designed to handle the truncation problem: (1) a lowering of the energy gap between the 0p and 1s0p shells, (2) a lowering of the $4\hbar\omega$ excitations alone, and (3) a removal of the SU3(20) symmetry component from the $V^{2\hbar\omega}$ interaction used in the diagonalization in the $(0+2+4)\hbar\omega$ model space, and a compensation for this omission by including perturbatively the (20) component in the effective operators used to calculate electroweak observables.

The second problem is that single-particle excitations through two oscillator shells must be included for the proper elimination of spurious center-of-mass motion, but one must maintain a proper balance

between the potential and kinetic energy contributions to the off-diagonal matrix elements connecting the $(n+2)\hbar\omega$ and $n\hbar\omega$ excitations. Also, single-particle self-consistency and the use of a saturating effective interaction are important to place the centroid of the monopole strength at a reasonable position (~ 20 - 30 MeV) ^{6,7}. For many applications, an adequate solution to this problem is to suppress these excitations except for that part needed to insure removal of spuriousity. This is the approach adopted by Haxton and Johnson ² and by us.

Shell-model calculations were performed with the shell-model code OXBASH ⁸. With Oxbash, spurious center-of-mass motion is removed by the usual method ⁹ of adding a center-of-mass Hamiltonian H_{cm} to the interaction. The shell-model studies use the recently constructed WBT and WBP Hamiltonians of Warburton and Brown discussed in another contribution.

An $n\hbar\omega$ excitation can contain contributions from ΔQ [$Q = 2N + 1$] nucleonic transitions with $\Delta Q \leq n$. Thus, with the $0\hbar\omega$ ^{16}O ground state taken as $0s_{1/2}^4 0p^{12}$ in the zeroth-order approximation, a $4\hbar\omega$ excitation involves the six lowest oscillator shells. Consequently interactions based on the four-shell WBT and WBP interactions were constructed in a six-shell model space. Our approach to the construction of this model space is essentially identical to that of Haxton and Johnson ². Namely, all $\Delta Q > 1$ TBME were set equal to zero. For ^{16}O this is equivalent to setting all $\Delta Q > 0$ TBME outside the basic $0p1s0d$ model space equal to zero. Thus the Hartree-Fock condition is satisfied and the $0s$ and 4 - 6 th shells are present for the sole purpose of allowing accurate removal of spurious center-of-mass motion. We began our shell-model studies by diagonalizing the 0^+ $T = 0$ and $0^- - 3^-$ $T = 1$ states of ^{16}O in both six-shell and four-shell model spaces. Negligible difference was found in the wave functions and observables of interest here as calculated within these two model spaces. This is not unexpected since the four-shell space is complete for $2\hbar\omega$ excitations and the $4\hbar\omega$ components in the low-lying states are largely $(0p)^{-4}(1s, 0d)^4$, and these $4p$ - $4h$ excitations as well as $2 \times (\Delta Q = 2)$ excitations are also allowed in the four-shell model space. The dimension $D(J^\pi)$ of the 0^+ states in the two model spaces differ negligibly — 4340 and 4255, respectively — but the four-shell model space is convenient in other ways. Thus some of the calculations reported here were performed in a four-shell model space — but, we emphasize that the results in a six-shell model space would be essentially identical.

Haxton and Johnson ² used a variant of the Millener-Kurath interaction ¹⁰ for the $0p1s0d$ model space and adjusted the four single-particle variables of this space to fit six low-lying $T = 0$ states in ^{16}O .

These four variables can be taken as the $0p_{3/2} - 0p_{1/2}$, $0d_{3/2} - 0d_{5/2}$, $1s_{1/2} - 0d_{5/2}$ and $0p_{1/2} - 0d_{5/2}$ energy splittings. The last of these we term the $0p$ - $1s0d$ energy gap $\Delta_{p,s,d}$. In our variant of the Haxton-Johnson method we keep the first three of these splittings fixed at the WBT values and vary $\Delta_{p,s,d}$ so as to place the 0_2^+ state ~ 6050 keV above the 0_1^+ state. We believe this one-parameter model contains the essence of the Haxton-Johnson four-parameter method. The necessary change in $\Delta_{p,s,d}$ was from 11632 keV in the four-shell WBT interaction to $11632 - 3020 = 8612$ keV. The odd-parity $T = 1$ states were calculated in a $(1+3)\hbar\omega$ model space using the same value of $\Delta_{p,s,d}$. This places the lowest predominantly $3\hbar\omega$ states ~ 5 MeV above the yrast states.

One obvious fault in the Energy-Gap method is that the $2\hbar\omega$ states receive a double lowering, first by $2 \times (11.632 - \Delta_{p,s,d})$ and again via the repulsive interaction with the $4\hbar\omega$ states. An obvious method which avoids this weakness is to lower the $4\hbar\omega$ components only. Then, this lowering can be viewed as the collective repulsive effect of $>4\hbar\omega$ excitations and should be roughly equal to the difference in binding of the ^{16}O ground state between $0\hbar\omega$ and $(0 + 2 + 4)\hbar\omega$ calculations. In OXBASH the total SPE contributions of different configurational components (partitions of nucleons between the available orbits) are calculated separately, thus it is straightforward to assign different energy gaps to different $n\hbar\omega$ excitations. For the WBT interaction, it is found that a shift $\Delta_{4\hbar\omega}$ of -10.90 MeV places the 0_2^+ state at 6.05 MeV excitation at the same time as the ground state is lowered 10.60 MeV from the $0\hbar\omega$ value. The close agreement in these shifts is evidence for the consistency of this method. The $\Delta_{4\hbar\omega}$ found for the WBP interaction is -10.10 MeV. Because diagonalization in a $5\hbar\omega$ space is beyond our capabilities, the odd-parity states cannot be treated in as logical a fashion and we simply use the same procedure for the odd-parity states as described for the energy-gap method.

The $\text{SU3}(20)$ component of $V^{2\hbar\omega}$ was set equal to zero by transforming from the jj -coupling basis used in OXBASH to a SU3 basis, setting all (20) TBME equal to zero and transforming back again. With all other TBME the same as in the WBT interaction, diagonalization in the four-shell model space produced a $(0+2+4)\hbar\omega$ ground state depressed by 2.7 MeV relative to a $0\hbar\omega$ calculation as compared to a depression of 10.6 MeV with the (20) symmetry included. With $\Delta_{4\hbar\omega} = -2.7$ MeV, the $4\hbar\omega$ first-excited state lies at 6005 keV.

The $\hbar\omega$ composition of the 0^+ states of ^{16}O obtained in the present calculations have been compared to each other and to those reported by Haxton and Johnson ² and Brown and Green ¹. We note some

relevant comparisons (a) The full $(0+2+4)\hbar\omega$ results of Haxton and Johnson are quite similar to the present Energy Gap results. (b) The Energy Gap method gives more $0\hbar\omega$ and $2\hbar\omega$ mixing in the ground state than the $\Delta_{4\hbar\omega}$ method. This is expected because of the explicit lowering of $2p-2h$ configurations in the Energy Gap method. (c) The SU3(20) method is closest to the Brown-Green method. This is expected because both are truncated so as to emphasize mixing between the first few 0^+ states, i.e., the SU3(20) method is the microscopic equivalent of the schematic Brown-Green model, in which only the SU3(42) tensor part of $V^{2\hbar\omega}$ acts between states with $\Delta\hbar\omega=2$. (d) The $2\hbar\omega$ components of the 0_1^+ and 0_2^+ states bear little resemblance to each other in either the $\Delta_{4\hbar\omega}$ or the Gap calculation. This is because the main $2\hbar\omega$ admixture in the ground state is of SU3(20) character while that in the $4\hbar\omega$ state is of SU3(42) character [the SU3(20) states have no matrix element with the “deformed” $4p-4h$ state which has (84) symmetry in the SU3 limit]. (e) The SU3(20) method gives much less configuration mixing than is obtained in the full $(0+2+4)\hbar\omega$ diagonalizations. From this we conclude that a first-order perturbation treatment does not work well in this case. However, we feel that the SU3(20) method may be useful in other nuclei where $4\hbar\omega$ excitations are not so important.

a. Brookhaven National Laboratory, Upton, New York 11973

References

1. G. E. Brown and A. M. Green, Nucl. Phys. 75, 401 (1966).
2. W. C. Haxton and C. Johnson, Phys. Rev. Lett. 65, 1325 (1990).
3. P. J. Ellis and L. Zamick, Ann. Phys. (N.Y.) 55, 61 (1969).
4. E. K. Warburton, D. E. Alburger, J. A. Becker, B. A. Brown, and S. Raman, Phys. Rev. C. 34, 1031 (1986).
5. E. K. Warburton, J. A. Becker, and B. A. Brown, Phys. Rev. C 41, 1147 (1990).
6. D. J. Millener, A. C. Hayes, and D. D. Strottman, Phys. Rev. C 45, 473 (1992).
7. T. Hoshino, H. Sagawa, and A. Arima, Nucl. Phys. A481, 458 (1988).
8. B. A. Brown, A. Etchegoyen, W.D.M. Rae, and N. S. Godwin, OXBASH, 1984 (unpublished).
9. D. H. Glockner and R. D. Lawson, Phys. Lett. 53B, 313 (1974).
10. D. J. Millener and D. Kurath, Nucl. Phys. A255, 315 (1975).

GAMOW-TELLER STRENGTH IN THE β^+ DECAY OF ^{37}Ca

B. A. Brown

It was recently proposed¹ that the analysis of new ^{37}Ca β^+ decay data called into question the extent to which the weak axial-vector current is renormalized in nuclei. This conclusion was based on the fact that the GT decay strength extracted from the new data was about equal to that obtained from a shell-model calculation with the free-nucleon value for $\lambda = g_A/g_V$ of 1.26. It was also claimed that this result cast some doubt on previous conclusions that the experimental GT strength for nuclei with $A=17-39$ was systematically quenched to only about 60% of that expected from $1s0d$ shell-model calculations.² I have shown that the quenching extracted from the ^{37}Ca β^+ decay data is more model dependent than most previous analyses of GT data. In particular, I have shown that it depends on the shape of the assumed GT strength distribution and that this shape is particularly sensitive to the Hamiltonian chosen for the $1s0d$ shell valence shell-model space. My discussion will also include additional information for the GT strength obtained from (p,n) data³ for the mirror transitions $^{37}\text{Cl} \rightarrow ^{37}\text{Ar}$. (Based upon calculations with charge-symmetry breaking interactions,⁴ the mirror symmetry breaking effects on the GT strengths are found to be not important for the discussion below.)

In Fig. 1 the $B(GT_+)$ strength extracted from the ^{37}Ca β^+ decay and from the (p,n) data (dashed lines) is compared with $1s0d$ shell-model calculations based upon four different effective Hamiltonians (solid lines). In order to emphasize the qualitative aspects of the comparison, what is shown is the $B(GT_+)$ strength vs excitation energy averaged over a Gaussian distribution with a FWHM of 2 MeV. The area under each curve is equal to the total $B(GT_+)$ strength. The experimental data up to about 8 MeV (the vertical dashed line in Fig. 1) is from the ^{37}Ca β^+ decay (Table 1 of Ref 5). Above 8 MeV the $B(GT)$ for states at 9.65 MeV and 11.5 MeV inferred from the (p,n) reaction on the mirror nucleus ^{37}Cl (Table I of Ref 3) is also included.

Two solid lines are given for each theoretical calculation in Fig. 1. The upper lines are based upon the free-nucleon value of $|\lambda| = 1.26$ and the areas under these upper lines are equal to the sum-rule value of $3\lambda^2 |N_i - Z_i| = 14.1$ [$B(GT_-)=0$ for ^{37}Ca in the $1s0d$ model space]. These results will be referred to as the "free-nucleon" calculations. The lower solid lines are based upon the state- and mass-dependent effective GT operator of Ref 2. For $A=37$ this effective operator is within a few percent the same as using a value of $|\lambda| = 0.90$, and the areas under all four of the lower lines are about 7.3. These results will be

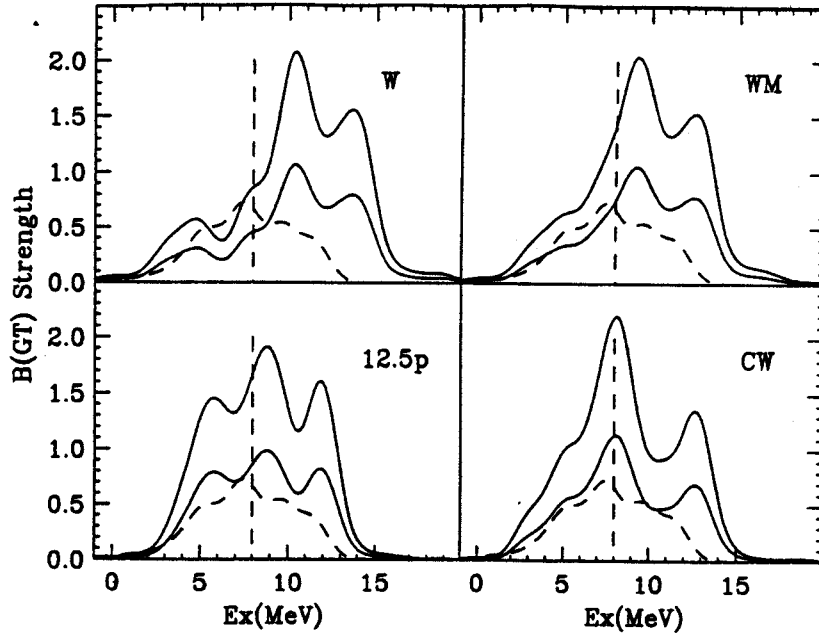


Figure 1: $B(GT_+)$ strength distribution for ^{37}Ca . The dashed line is the strength extracted from experiment, and the solid lines correspond to various theoretical calculations (see text for details).

referred to as the “quenched” calculations. A different effective Hamiltonian was used for each of the four comparisons made in Fig. 1.

The calculation in bottom-left is based upon a microscopic G matrix interaction plus core-polarization corrections (The column labeled 12.5p in Table 1 of Ref 6). The calculation in the bottom-right is based upon the Chung-Wildenthal (CW) “hole” Hamiltonian.⁷ The CW Hamiltonian was obtained from a least-squares fit of binding-energy data for nuclei in the $A=32-39$ region with the least well determined linear combinations of two-body matrix elements being kept at the 12.5p values. In both cases the single-hole energies are chosen to give excitation energies of 2.50 MeV ($1s_{1/2}$) and 6.12 MeV ($0d_{5/2}$) relative to the $0d_{3/2}$ ground state of $A=39$. The calculation shown at the top-left is based upon Wildenthal’s (W) Hamiltonian.⁸ The W Hamiltonian started with the Chung-Wildenthal “particle” ($A=17-24$) and “hole” ($A=32-39$) Hamiltonians and made further adjustments so that 447 binding-energy data across the entire $1s0d$ shell ($A=17-39$) were reproduced with an rms deviation of 185 keV.^{8,9} 47 linear combinations of the 66 Hamiltonian parameters were relatively well determined by these data.^{8,9} With the W Hamiltonian, the $A=39$ single-hole states come at 2.73 MeV ($1s_{1/2}$) and 7.42 MeV ($0d_{5/2}$). The $0d_{5/2}$ single-hole energy is significantly higher for the W Hamiltonian than for the CW Hamiltonian. The W Hamiltonian was constrained to reproduce a specific value for the energy of the $A=39$ $0d_{5/2}$ hole state, however, it turns out

that the energy obtained with the W Hamiltonian is in good agreement with the centroid of the strength observed in one-nucleon pickup from ^{40}Ca .¹⁰ The spectrum labeled WM on the top-right was obtained from the W interaction interaction but with the single-particle energies adjusted to give the same single-hole energies as CW.

The claim of “no quenching” by Adelberger et al.,¹ is based upon the fact that the areas below 8 MeV under the experimental (dashed line) and the free-nucleon W calculation (upper solid line) in the top-left part of Fig. 1 are about equal to each other. However, it is apparent that only a small part (20%) of the theoretical strength lies below 8 MeV and that the comparison is thus very sensitive to what one assumes for the shape of the strength distribution. If one takes the $^{37}\text{Cl}(p,n)$ data as an indication of the shape of the remaining strength, it is clear that the shape of the total data is much closer to the 12.5p or CW calculations than to the W calculation. When compared to the 12.5p or CW calculations, the interpretation of the data below 8 MeV from the beta decay is that it is consistent with the effective (quenched) GT operator (lower-lines).

Furthermore, it is apparent that the absolute strength obtained from the (p,n) data above 8 MeV is about a factor of two smaller than the quenched calculation. One aspect of the non-proportionality between GT strength extracted from beta decay, $B(GT)_\beta$ and (p,n) experiments, $B(GT)_{pn}$, has previously been noted.¹¹ In particular, the ratio $B(GT)_{pn}/B(GT)_\beta$ for transitions between “jackknife” configurations ($p_{1/2} \rightarrow p_{1/2}$ and $d_{3/2} \rightarrow d_{3/2}$, in particular) was found to be systematically larger than that between “spin-flip” transitions ($0d_{3/2} \rightarrow 0d_{5/2}$ in this case). The implication of this is that if one calibrates the (p,n) reaction to low-lying transitions with a jackknife structure, the strength extracted for the high-lying spin-flip transitions is too small. A recalibration of the old $^{37}\text{Cl}(p,n)^{37}\text{Ar}$ data and new higher-resolution data would be important for testing this hypothesis. It would also be important to measure the GT strength above 12 MeV in excitation in ^{37}Ar . The proportionality between GT strength extracted from (p,n) reactions and beta decay must eventually break down for transitions which are very weak (a few percent or less) relative to the sum rule value (transitions to the lowest few $A=37$, $T=1/2$ levels in this case). There are, of course, additional experimental problems and uncertainties in subtracting the Fermi strength in transitions to analog states (the 5.05 MeV final state in this case).

The problem with the position of the GT strength with the W Hamiltonian is primarily in the upper part of the $1s0d$ shell; GT strength distributions observed in (p,n) reactions for nuclei in the lower

and middle parts of the $1s0d$ shell ($A=18-32$) are in overall good agreement with the W Hamiltonian [Ref 8 and references therein]. In fact, for $A=18$ and 19 there are several cases where most of the GT strength resides in low-lying levels which are directly populated in mirror beta decay² and whose energies were integral in determining the W Hamiltonian. Thus, the previous conclusions concerning the quenching of GT strength,² which are based primarily on β decay data in the lower and middle parts of the $1s0d$ shell, are still valid. In addition, I point out that the quenching obtained from the ^{39}Ca β^+ decay² and the $^{39}\text{K}(p,n)$ data¹¹ is completely independent of the $1s0d$ Hamiltonian. A further evolution of the $1s0d$ -shell Hamiltonian which would incorporate both the success of the W Hamiltonian across the shell and the CW interaction for the GT distribution in the upper part of the shell will remain a challenge.

References

1. E. G. Adelberger, A. Garcia, P. V. Magnus and D. P. Wells, Phys. Rev. Lett. 67, 3658 (1991).
2. B. A. Brown and B. H. Wildenthal, At. Data Nucl. Data Tables 33, 347 (1985).
3. J. Rapaport et al., Phys. Rev. Lett. 47, 1518 (1981).
4. W. E. Ormand and B. A. Brown, Nucl. Phys. A491, 1 (1989).
5. A. Garcia et al., Phys. Rev. Lett. 67, 3654 (1991).
6. B. H. Wildenthal et al., Phys. Rev. C4, 1266 (1971).
7. W. Chung, Phd. Thesis, Michigan State Univ., 1976; B. H. Wildenthal and W. Chung in "Mesons in Nuclei" Vol. II, edited by M. Rho and D. Wilkinson (North-Holland, 1979).
8. B. A. Brown and B. H. Wildenthal, Annu. Rev. Nucl. Part. Sci. 38, 29 (1988).
9. B. A. Brown et al., Ann. Phys. 182, 191 (1988).
10. P. Doll et al., Nucl. Phys. A263, 210 (1976).
11. J. W. Watson et al., Phys. Rev. Lett. 55, 1369 (1985).

MOMENTUM DISTRIBUTIONS IN RADIOACTIVE BEAM INTERACTIONS

C.A. Bertulani and K.W. McVoy^a

We investigate the longitudinal and transverse momentum distributions of charged fragments originating from reactions with radioactive, neutron-rich, beams. It is shown ¹ that the width of the narrow peak of the longitudinal momentum distribution is insensitive to the details of the collision and the size of the target nucleus. This peak is primarily sensitive to the separation energy, or halo size, of the loosely-bound projectile neutrons, and should provide a reliable measure of this quantity.

In contrast, the width of the peripheral region from which transversely moving particles originate is significantly narrowed via absorption of the outgoing neutrons. This diffractively broadens the width of their transverse momentum distribution, in a manner which depends on details of the collision, and so makes the transverse distribution less reliable than the longitudinal one for measuring the size of the original neutron halo.

a. Physics Department, University of Wisconsin, Madison, Wisconsin 53706

References

1. C.A. Bertulani and K.W. McVoy, submitted to Phys. Lett. B.

SEMICLASSICAL CALCULATION OF COULOMB BREAK-UP OF WEAKLY-BOUND NUCLEI

C.A. Bertulani and L.F. Canto^a

We develop ¹ a semiclassical coupled-channels calculation for the Coulomb break-up of loosely-bound nuclei. The continuum wavefunctions are discretized by means of two different sets of strongly peaked functions: (a) a histogram set, and (b) a continuously derivable one. Using simple expressions for the bound- and continuum-wavefunctions, we calculate the break-up probability to first-order and with the coupled-channels method. First-order perturbation theory is shown to fail to describe the Coulomb break-up of unstable projectiles, as ¹¹Li at small impact parameters. It is shown that a non-perturbative calculation may reduce the cross section by 20% in collisions at intermediate energies.

a. Instituto de Física, Universidade Federal do Rio de Janeiro, 21945, Rio de Janeiro, RJ, Brazil

References

1. C.A. Bertulani and L.F. Canto, Nucl. Phys. A539 (1992) 163

NUCLEON-NUCLEON CORRELATION EFFECTS IN THE ELASTIC SCATTERING OF α -PARTICLES FROM ^{11}Li AT 26 MeV/NUCLEON

A.N.F. Aleixo^a, C.A. Bertulani and M.S. Hussein^b

Recently, the elastic scattering of different nuclei from ^{11}Li has been calculated ^{1,2,3}. The motivation for this interest is connected with the possible encountering of a signature of the neutron halo in the elastic angular distribution and the need of elastic information to study quasi-elastic processes. Experimental programs to investigate these processes are already underway ⁴. Further investigation of the elastic scattering involving ^{11}Li is certainly required to better understand the average nuclear interaction.

We extended our study ² of $p + ^{11}\text{Li}$ to the case of $\alpha + ^{11}\text{Li}$. The tightly bound α -particle should prove an interesting probe as it represents, at low energies, a heavier charged "nucleon". To what extent the halo of ^{11}Li is sensitive to the size of the impinging particle, is a question that can be partly answered by comparing the two systems $p + ^{11}\text{Li}$ and $\alpha + ^{11}\text{Li}$ at relatively low energies. We take this energy to be $E_{Lab} = 26 \text{ MeV}$, since precise data ⁵ on the elastic scattering of p from α exist and can be used to extract the $p - \alpha$ optical potential. This potential is then used to calculate the $\alpha - ^{11}\text{Li}$ single folding optical potential. Since the energy is too low for the usual ⁶ single-folding approximation to the potential to be valid, we also calculate the second order contribution which carry important information about nucleon-nucleon short range correlations in the nucleus ⁷.

- a. Instituto de Física, Universidade Federal do Rio de Janeiro 21945, Rio de Janeiro, RJ, Brazil
- b. Nuclear Theory and Elementary Particle Phenomenology Group, Instituto de Física, Universidade de São Paulo, C.P. 20 516, 01498 São Paulo, SP, Brazil

References

1. G. R. Satchler, K. W. McVoy and M. S. Hussein, Nucl. Phys. A522 (1991) 621
2. A. N. F. Aleixo, C. A. Bertulani and M. S. Hussein, Phys. Rev. C43 (1991) 2722
3. Y. Hirabayashi, S. Funada and Y. Sakuragi, Contribution to the Symposium on Structure and Reactions of Unstable Nuclei, June 17-19, 1991, Niigata, Japan, p.23.
4. J. Kolata, private communication.
5. D. J. Plummer *et al.*, Nucl. Phys. A174 (1971) 193
6. M. S. Hussein, R. A. Rego and C. A. Bertulani, Phys. Rep. 201 (1991) 279
7. A.N.F. Aleixo, C.A. Bertulani and M.S. Hussein, Phys. Rev. C45 (1992) 2403

CLOSED FORM THEORY OF ELASTIC BREAKUP AND APPLICATIONS TO ASTROPHYSICALLY RELEVANT HEAVY ION REACTIONS

C.A. Bertulani, L.F. Canto^a and M.S. Hussein^b

Break-up reactions constitute an important piece of the total reaction cross section of intermediate energy heavy ion collisions. It is now quite common to separate the break up process into two physically distinct processes: elastic break-up, and inclusive inelastic break-up (also called break-up fusion). Whereas semi-analytical treatments of the latter process have been extensively developed ¹, only numerical recipes based on either post or prior DWBA description are available in the literature. Elastic break-up reactions are of great importance since it represents an appreciable part of the total break-up cross section. Furthermore, it can be used as a vehicle through which fusion cross section of light-heavy ions at extremely low energies, of great relevance to astrophysical research, can be extracted through detailed balance arguments ^{2,3}. The above fact clearly calls for more theoretical analysis of the elastic break-up process in order to render the numerics simpler.

We developed a semi-analytical treatment of the elastic break-up cross section. In this endeavor, we rely heavily on the work of Frahn ⁴, who considered heavy ion inelastic and transfer reactions at low energies. The approximations he employed are, in fact, more valid at the higher energies we consider here since they are, based to some extent, on the eikonal method. We apply our theory ⁵ to some recent data on the reaction $^{16}\text{O} + ^{28}\text{Si} \rightarrow \alpha + ^{12}\text{C} + ^{28}\text{Si}$ at 4 MeV $\cdot A$ and find reasonable agreement.

- a. Instituto de Física, Universidade Federal do Rio de Janeiro, C.P. 68528, 21945 Rio de Janeiro, RJ, Brazil
- b. Nuclear Theory and Elementary Particle Phenomenology Group, Instituto de Física, Universidade de São Paulo, C.P. 20516, São Paulo, SP, Brazil

References

1. M.S. Hussein and K.W. McVoy, Nucl. Phys. A445 (1985) 124
2. G. Baur, C.A. Bertulani and H. Rebel, Nucl. Phys. A459 (1986) 188;
G. Baur, C.A. Bertulani and H. Rebel, Proc. Int. Symp. on Weak and Electromagnetic Interactions in Nuclei, July 1-5, 1986, Heidelberg, Germany, ed. H.V. Klapdor (Springer, Berlin, 1986) p. 980
3. T. Motobayashi et al., Phys. Lett. B264 (1991) 259;
J. Kiener et al., Phys. Rev. C44 (1991) 2195
4. W.E. Frahn, Phys. Rev. C21 (1980) 1870
5. C.A. Bertulani, L.F. Canto and M.S. Hussein, Phys. Rev C, in press

EXCITATION AND GAMMA-DECAY OF HEAVY IONS IN HIGH ENERGY COLLISIONS

C.A. Bertulani and A.M. Nathan^a

There has been interest in recent years in the study of photon decay of the Giant Dipole Resonance (GDR). Until recently, these studies have utilized the photon scattering reaction. An alternate method has now emerged in which heavy ion collisions are used to electromagnetically excite the nucleus to the GDR (via Coulomb excitation) and the subsequent decay photons are observed. In effect, this is just photon scattering where the incident photon is virtual. We have been investigating whether the connection between these two reactions can be formalized. In the process, we have developed closed-form expressions for the cross section for the electromagnetic excitation induced by heavy ion collisions at intermediate and high energies. These expressions directly relate the excitation cross section to the corresponding photonuclear cross section. When applied to the excitation/photon decay process, we obtain a result that differs in a fundamental way from that traditionally used to interpret the Coulomb excitation/photon decay data.

The physical situation is that of a heavy ion of energy E incident on a target. The projectile loses an energy ΔE while scattering through an angle θ . Under the conditions $\Delta E/E_{lab} \ll 1$ and $\theta \ll 1$, the cross section for excitation of the target nucleus neatly partitions to the following expression:

$$\frac{d\sigma_C}{d\Omega}(E_\gamma) = \frac{1}{E_\gamma} \frac{dn_\gamma}{d\Omega} \sigma_\gamma(E_\gamma) \quad (1)$$

where $\sigma_\gamma(E_\gamma)$ is the photonuclear cross section for the absorption of a real photon with energy $E_\gamma = \Delta E$ by the target nucleus, and $dn_\gamma/d\Omega$ is the number of virtual photons with energy E_γ . This latter quantity depends on the kinematics of the scattered heavy ions and on the optical potential but is otherwise independent of the target degrees of freedom. This partitioning allows one to relate the excitation cross section to the photoabsorption cross section. Now, the standard way to write the cross section $d\sigma_C/d\Omega$ for the excitation of the target followed by photon decay is simply to multiply the above expression by a branching ratio R_γ , which represents the probability that the nucleus excited to an energy E_γ will emit a photon leaving it in the ground state:

$$\frac{d\sigma_C}{d\Omega}(E_\gamma) = \frac{1}{E_\gamma} \frac{dn_\gamma}{d\Omega} \sigma_\gamma(E_\gamma) R_\gamma(E_\gamma). \quad (2)$$

Instead, we propose the following expression:

$$\frac{d\sigma_C}{d\Omega}(E_\gamma) = \frac{1}{E_\gamma} \frac{dn_\gamma}{d\Omega} \sigma_{\gamma\gamma}(E_\gamma) \quad (3)$$

where $\sigma_{\gamma\gamma}$ is the cross section for the photon scattering at energy E_γ . These expressions would be equivalent to each other if it were true that the photon scattering cross section is just the photoabsorption cross section times a branching ratio. In fact, it is not true. In particular, it is not correct to think of photon scattering as a two-step process of excitation to a definite energy followed by photon decay. We have exploited our formalism for the analysis and interpretation of Coulomb excitation/photon decay data^{1,2}. The results of this analysis will be published elsewhere³.

a. Nuclear Physics Laboratory GL-10, University of Washington, Seattle, WA 98195

References

1. J. Barrete *et al.*, Phys. Lett. B209 (1988) 182
2. J.R. Beene *et al.*, Phys. Rev. C41 (1990) 920
3. C.A. Bertulani and A.M. Nathan, MSU-preprint 1992, submitted to Nucl. Phys. A.